

GLOBAL AND LOCAL HELICITY-PRESERVATION IN THE FINITE ELEMENT DISCRETISATION OF MAGNETIC RELAXATION *

PATRICK E. FARRELL[†], MINGDONG HE[‡], KAIBO HU[§], AND GANGHUI ZHANG[¶]

Abstract. Magnetic relaxation drives plasma toward lower-energy equilibria under helicity constraints. In ideal magnetohydrodynamics (MHD), helicity is locally conserved, while resistive theories such as Taylor relaxation preserve only global helicity. This distinction has important implications for structure-preserving numerical methods. We compare three finite element formulations: an unconstrained scheme that does not conserve helicity, a mixed method based on finite element exterior calculus that preserves all local helicities, and a Lagrange multiplier approach that enforces only global helicity conservation. Numerical experiments on braided and knotted magnetic fields show that local helicity preservation prevents spurious reconnection and maintains nontrivial topology in ideal MHD or magneto-friction, whereas enforcing only global helicity allows further relaxation through local reconnection. Numerical results on magnetic knots and braids are provided. These results clarify how different levels of discrete helicity constraints influence magnetic relaxation and equilibrium structure in numerical computation.

Key words. magnetohydrodynamics, structure-preservation, Lagrange multiplier, finite element exterior calculus, magnetic helicity, magnetic relaxation.

MSC codes. 65N30, 65L60, 76W05

1. Introduction. Magnetic relaxation describes the process by which a magnetized plasma reorganizes its magnetic field toward a lower-energy equilibrium. Magnetic relaxation is a fundamental process in plasma physics, playing a central role in the understanding of magnetic equilibria in both natural and laboratory plasmas. In magnetically ideal situations, this reorganization is described by the ideal magnetohydrodynamic (MHD) equations, or their simplification, the magneto-frictional (MF) equations [15, 28, 45, 51] posed on a bounded, contractible, Lipschitz domain $\Omega \subset \mathbb{R}^3$:

$$\begin{aligned} (1.1a) \quad & \partial_t \mathbf{B} + \nabla \times \mathbf{E} = \mathbf{0}, \\ (1.1b) \quad & \mathbf{E} + \mathbf{u} \times \mathbf{B} = \mathbf{0}, \\ (1.1c) \quad & \mathbf{u} = \tau \mathbf{j} \times \mathbf{B}, \\ (1.1d) \quad & \mathbf{j} = \nabla \times \mathbf{B}, \end{aligned}$$

*Submitted to the editors DATE.

Funding: This work was funded by the Engineering and Physical Sciences Research Council [grant number EP/W026163/1], the Science and Technology Facilities Council [grant number UKRI/ST/B000495/1], the Donatio Universitatis Carolinae Chair “Mathematical modelling of multicomponent systems”, the UKRI Digital Research Infrastructure Programme through the Science and Technology Facilities Council’s Computational Science Centre for Research Communities (CoSeC), the Swedish Research Council under grant no. Z2021-06594 while in residence at Institut Mittag-Leffler in Djursholm, Sweden, the European Research Council (ERC Starting Grant, project 101164551 GeoFEM), and by a Royal Society University Research Fellowship (URF\R1\221398). For the purpose of open access, the authors have applied a CC BY public copyright licence to any author accepted manuscript arising from this submission. No new data were generated or analysed during this work.

[†]Mathematical Institute, University of Oxford, UK and Mathematical Institute, Faculty of Mathematics and Physics, Charles University, Czechia (patrick.farrell@maths.ox.ac.uk)

[‡]Mathematical Institute, University of Oxford, UK (mingdong.he@maths.ox.ac.uk)

[§]Mathematical Institute, University of Oxford, UK (kaibo.hu@maths.ox.ac.uk)

[¶]Mathematical Institute, University of Oxford, UK (ganghui.zhang@maths.ox.ac.uk)

where \mathbf{B} is the magnetic field, \mathbf{E} is the electric field, \mathbf{u} , is the velocity, \mathbf{j} is the current, and $\tau > 0$ is a coupling parameter. These MF equations possess the same equilibria as the ideal MHD equations, allowing their study with less computational expense.

Both the ideal MHD and MF systems impose topological constraints of the magnetic fields. Helicity is a quantitative measure of the knottedness and linking of the magnetic fields, which is defined on a domain $\Omega_s \subset \Omega$ as

$$(1.2) \quad \mathcal{H}(\Omega_s) := \int_{\Omega_s} \mathbf{A} \cdot \mathbf{B} \, dx,$$

where \mathbf{A} is any magnetic potential satisfying $\nabla \times \mathbf{A} = \mathbf{B}$. The quantity $\mathcal{H}(\Omega)$, known as Woltjer's invariant [49], describes the total averaged knotting of the magnetic field in the domain. Hereafter, we refer to this quantity as the *global* helicity since it is integrated over the entire domain. Woltjer's invariant is conserved in ideal MHD. In fact, $\mathcal{H}(\Omega_s)$ is conserved for any *magnetically closed domain* $\Omega_s \subset \Omega$, i.e., any subdomain Ω_s such that \mathbf{B} is tangent to its boundary ($\mathbf{B}|_{\partial\Omega_s} \cdot \mathbf{n}_{\partial\Omega_s} = 0$). A more geometric description is that the volume form $\mathbf{A} \wedge \mathbf{B}$ is transported by the flow and is thus invariant. Hereafter, we refer to the conservation of $\mathcal{H}(\Omega_s)$ for $\Omega_s \subsetneq \Omega$ as the *local* conservation of helicity. In both ideal MHD and the MF equations, the local helicity is conserved in time for any suitable Ω_s . For a comprehensive review of magnetic relaxation and its topological constraints, we refer to [50].

Numerical simulations of magnetic relaxation yield nonphysical results if the numerical schemes do not appropriately preserve helicity [28]; if helicity is not conserved, then the magnetic field relaxes without topological constraints towards the trivial zero state $\mathbf{B} = \mathbf{0}$. In our previous work [28] we introduced a structure-preserving scheme. However, this scheme requires the introduction of auxiliary variables (fields over the domain), and is substantially more expensive than non-structure-preserving approaches. In this work we investigate whether this is necessary: to predict the correct relaxed state, is it possible to use a cheaper real-valued Lagrange multiplier to preserve $\mathcal{H}(\Omega)$? Realizing the distinction between local and global helicities, we reframe the central question as follows: to recover the physically relevant relaxed state, is conservation of global helicity alone adequate (as achieved by a Lagrange-multiplier approach), or must both the global helicity and all local helicities be preserved, as imposed in the mixed-variable structure-preserving scheme [28]?

We therefore compare three finite element discretizations. The first takes no special care to conserve helicity on discretization and leads to nonphysical trivial states. The second is our projection-based scheme from [28], which introduces the projection of the magnetic field onto another function space so as to conserve helicity for every magnetically closed domain. The third is a novel scheme where the global helicity constraint is enforced with a Lagrange multiplier. This corresponds to Taylor's relaxation theory [38, 45], which assumes that the global helicity is approximately conserved in the real plasma relaxation, although local helicities can change due to reconnections. The first leads to $\mathbf{B} = \mathbf{0}$ and thus with vanishing current $\mathbf{j} = \nabla \times \mathbf{B} = \mathbf{0}$; the second leads to so-called 'nonlinear force-free fields' with $\mathbf{j} = \alpha(\mathbf{x})\mathbf{B}$; the third leads to so-called 'linear force-free fields' with $\mathbf{j} = \alpha\mathbf{B}$ for a constant α . In the second and third cases, equilibrium is described by the vanishing of the Lorentz force

$$(1.3) \quad \mathbf{j} \times \mathbf{B} = \mathbf{0}.$$

We demonstrate that solving the MF equations with the Lagrange multiplier scheme leads to qualitatively wrong solutions: the magnetic field decays to zero due to

spurious numerical reconnections of the field lines. This evinces the crucial importance of *local*-helicity-preservation in problems where local helicity is preserved. For these problems, the numerical scheme enforcing only the global constraint is not enough to correctly compute the steady state with local topological structures. In fact, even for magnetic knots with non-zero helicity, the Lagrange multiplier scheme may still converge to different stationary states (though nonzero) compared to the projection-based approach (see [Figure 6.4](#) below).

However, real physical situations are not ideal, breaking helicity conservation. Taylor’s relaxation theory assumes that the global helicity is approximately conserved to high accuracy, although local helicities are not [\[38, 45, 50\]](#). A consequence of the Taylor relaxation theory is that turbulent plasmas relax toward a linear force-free state under only the global constraint. In the latter part of this paper, we discuss the possibility of using the local reconnections arising from numerical errors in the Lagrange multiplier approach as an approach for simulating Taylor relaxation. In short, *numerical errors (reconnections) in local helicity might reflect the reconnection of magnetic fields in the real physical problem, leading to physically relevant solutions.* The physics of magnetic relaxation can be a decisive factor for the choice of numerical schemes, especially at the level of helicity preservation.

Another important consideration in magnetic relaxation is its performance on a wider range of topological configurations. While nonzero helicity implies nontrivial topology (e.g. linked tubes or rings), the converse is not true: there can be topologically nontrivial magnetic fields with zero helicity. The analysis in [\[28\]](#) only applies to those fields with nonzero helicity, by proving a discrete Arnold inequality that guarantees a lower bound on the evolution of the magnetic energy. For topologically nontrivial fields with zero helicity, such as the magnetic braid E^3 -fields that are important models in solar physics, our numerical experiments demonstrate that the relaxed state obtained from [\[28\]](#) still has nontrivial topology.

More generally, the past decades have seen significant progress in finite element methods for MHD systems. In particular, schemes based on the finite element exterior calculus (FEEC) [\[3–5\]](#) have been developed that precisely preserve important structure, such as the magnetic Gauss law and helicity conservation [\[9, 19, 25, 29, 30, 33, 35, 36, 54, 55\]](#). Extensive numerical results demonstrate that standard finite element methods that do not explicitly enforce helicity conservation produce qualitatively wrong solutions, as discretization errors destroy topological structures, whereas helicity-preserving methods evolve toward physically meaningful solutions. While Lagrangian discretizations have been widely employed to track these constraints [\[11, 16–18, 34, 47, 48, 56–58\]](#), Eulerian discretizations have advantages in stability and the handling of complex geometries [\[9, 28\]](#).

The remainder of this paper is organized as follows. In [Section 2](#), we introduce preliminaries and the magnetic topologies we consider, including magnetic knots and magnetic braids. In [Section 3](#), we propose a non-conservative scheme based on a naïve formulation. The projected-based finite element method of [\[28\]](#) is reviewed and discussed in [Section 4](#). Then in [Section 5](#), we propose a global structure-preserving scheme via Lagrange multipliers. In [Section 6](#), we present numerical results, and compare the non-conservative scheme, the projection-based method, and the Lagrange multiplier method, to explore the significance of global and local helicity preservation. In [Section 7](#), we further discuss the background physical meaning of the two structure-preserving schemes. Finally we draw some conclusions in [Section 8](#).

2. Preliminaries: helicity and magnetic topology. Let Ω be a bounded Lipschitz domain in \mathbb{R}^3 ; if not otherwise specified, we assume that Ω is contractible. Let \mathbf{n} denote the outward-pointing unit normal vector on $\partial\Omega$. We use $\|\cdot\|$ and (\cdot, \cdot) to denote the $L^2(\Omega)$ norm and inner product respectively, allowing $L^2(\Omega)$ to denote both the scalar- and vector-valued spaces. The Hilbert spaces H^1 , $\mathbf{H}(\text{curl})$ and $\mathbf{H}(\text{div})$ are defined as in e.g. [3]. We further introduce subspaces H_0^1 , $\mathbf{H}_0(\text{curl})$ and $\mathbf{H}_0(\text{div})$ with homogeneous boundary conditions on $\partial\Omega$.

The 3D de Rham complex with homogeneous boundary conditions reads:

$$(2.1a) \quad 0 \longrightarrow H_0^1 \xrightarrow{\nabla} \mathbf{H}_0(\text{curl}) \xrightarrow{\nabla \times} \mathbf{H}_0(\text{div}) \xrightarrow{\nabla \cdot} L_0^2 \longrightarrow 0.$$

This complex (2.1a) is exact on contractible domains. We will use finite-element subcomplexes of (2.1a) for discretization; families of such subcomplexes are well-known, consisting of Nédélec [40], Raviart–Thomas [42], and Brezzi–Douglas–Marini elements [10], each extending to arbitrary spatial dimensions and polynomial degrees. Adopting the notation of [4], we denote such a subcomplex by

$$(2.1b) \quad 0 \longrightarrow H_0^{1,h} \xrightarrow{\nabla} \mathbf{H}_0^h(\text{curl}) \xrightarrow{\nabla \times} \mathbf{H}_0^h(\text{div}) \xrightarrow{\nabla \cdot} L_0^{2,h} \longrightarrow 0.$$

We require that (2.1b) is exact on contractible domains.

Define the magnetic energy

$$(2.2) \quad \mathcal{E} = \int_{\Omega} \mathbf{B} \cdot \mathbf{B} \, dx.$$

We always assume the whole domain Ω is a magnetic closed domain, and denote the global helicity $\mathcal{H} := \mathcal{H}(\Omega)$. The Arnold inequality [6] is a crucial result imposing a topological barrier on the energy achievable by magnetic relaxation. It states that

$$(2.3) \quad |\mathcal{H}| \leq C\mathcal{E},$$

for a constant $C > 0$. We close (1.1) with the boundary conditions

$$(2.4) \quad \mathbf{B} \cdot \mathbf{n} = 0, \quad \mathbf{j} \times \mathbf{n} = \mathbf{0}, \quad \mathbf{u} \cdot \mathbf{n} = 0, \quad \text{on } \partial\Omega,$$

which ensure that the magnetic energy \mathcal{E} decreases until reaching its equilibrium. The local helicity on any magnetic subdomain, and hence the global helicity, is conserved.

Magnetic fields can exhibit non-trivial topology, arising from the winding, linking, or tangling of magnetic field lines. A classic example is the magnetic knot, in which field lines form closed loops that are linked or knotted in a topologically non-trivial way. In contrast, magnetic braids consist of open flux tubes whose field lines are tangled between two boundaries (e.g., photospheric footpoints) but do not necessarily form closed, linked loops [53]. Because opposite twists can cancel, magnetic braids often possess zero net helicity. Consequently, the global helicity \mathcal{H} is insensitive to their internal topological complexity and fails to distinguish between different braiding patterns. Another example is the Borromean rings configuration, where the global helicity vanishes despite non-trivial triple linking.

This limitation of helicity in describing richer topological configurations inspires the investigation of other measures, such as higher-order linking invariants [7, 37] for configurations like the Borromean rings, and more refined, local, or field-line-based definitions, such as field-line mapping, topological entropy, or distributions of field-line

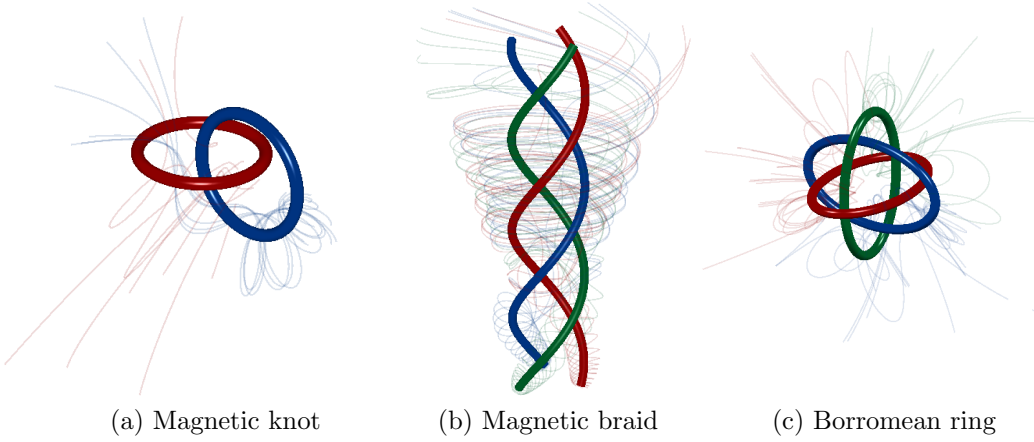


Fig. 2.1: Illustration of non-trivial topology of magnetic fields. (a) Magnetic knot with non-zero helicity, (b) Magnetic braid with zero helicity and (c) Borromean ring with zero helicity. Here the thin lines represent the magnetic field lines surrounding the high-intensity core tubes.

helicity, to describe braided topology [52, 53]. These quantities reveal local winding and stretching even when global helicity is zero. However, reflecting these structures in finite element computation is still largely open, and is beyond the scope of this paper.

The fundamental structural differences between magnetic knots (closed, helicity-carrying) and magnetic braids (open, often helicity-neutral yet topologically rich) provide striking test cases for helicity-preserving numerical schemes. We will investigate the dynamics of these topological configurations with algorithms for magnetic relaxation that enforce varying degrees of helicity conservation during energy minimization.

3. Non-conservative scheme. A natural discretization of the MF equations (1.1), (2.4) using variables from a de Rham complex follows from [30, 31].

PROBLEM 3.1 (Non-conservative scheme). *At time step $n \geq 0$, find*

$$(\mathbf{B}_h^{n+1}, \mathbf{E}_h^{n+1/2}, \mathbf{j}_h^{n+1/2}) \in [\mathbf{H}_0^h(\text{div})] \times [\mathbf{H}_0^h(\text{curl})]^2$$

such that for any test function $(\mathbf{C}_h, \mathbf{F}_h, \mathbf{k}_h) \in [\mathbf{H}_0^h(\text{div})] \times [\mathbf{H}_0^h(\text{curl})]^2$,

$$(3.1a) \quad \left(\frac{\mathbf{B}_h^{n+1} - \mathbf{B}_h^n}{\Delta t}, \mathbf{C}_h \right) + (\nabla \times \mathbf{E}_h^{n+1/2}, \mathbf{C}_h) = 0,$$

$$(3.1b) \quad (\mathbf{E}_h^{n+1/2}, \mathbf{F}_h) + \tau((\mathbf{j}_h^{n+1/2} \times \mathbf{B}_h^{n+1/2}) \times \mathbf{B}_h^{n+1/2}, \mathbf{F}_h) = 0,$$

$$(3.1c) \quad (\mathbf{j}_h^{n+1/2}, \mathbf{k}_h) - (\mathbf{B}_h^{n+1/2}, \nabla \times \mathbf{k}_h) = 0,$$

where we use the Crank–Nicolson temporal discretization method for \mathbf{B}_h , that is, $\mathbf{B}_h^{n+1/2} = (\mathbf{B}_h^{n+1} + \mathbf{B}_h^n)/2$, and consider $\mathbf{E}_h^{n+1/2}$ and $\mathbf{j}_h^{n+1/2}$ as independent variables. The scheme preserves the magnetic Gauss law $\nabla \cdot \mathbf{B} = 0$ and the energy decay.

THEOREM 3.2. *Assume $(\mathbf{B}_h^{n+1}, \mathbf{E}_h^{n+1/2}, \mathbf{j}_h^{n+1/2})$ is a solution of (3.1). Then the energy is decreasing and the discrete Gauss law holds, that is,*

$$(3.2) \quad \mathcal{E}_h^{n+1} \leq \mathcal{E}_h^n \leq \dots \leq \mathcal{E}_h^0,$$

and

$$\nabla \cdot \mathbf{B}_h^{n+1} = 0, \quad n \geq 0,$$

where $\mathcal{E}_h^n = (\mathbf{B}_h^n, \mathbf{B}_h^n)$.

However, the discrete helicity is not conserved at either the local or global level due to numerical pollution [29]. Moreover, the lack of the discrete Arnold inequality leads to nonphysical solutions, as shown in Section 6 below.

4. Projection-based mixed finite element scheme. We briefly review the model and schemes presented in [28]. The projection-based mixed finite element scheme (*projection-based scheme*, in short) in [28] introduces an additional auxiliary variable and conserves all local helicities. The system can be written as

$$(4.1a) \quad \partial_t \mathbf{B} + \nabla \times \mathbf{E} = \mathbf{0},$$

$$(4.1b) \quad \mathbf{E} + \mathbf{u} \times \mathbf{H} = \mathbf{0},$$

$$(4.1c) \quad \mathbf{j} = \nabla \times \mathbf{B},$$

$$(4.1d) \quad \mathbf{u} = \tau \mathbf{j} \times \mathbf{H},$$

$$(4.1e) \quad \mathbf{H} = \mathbf{B},$$

where $\mathbf{H} \in \mathbf{H}_0^h(\text{curl})$ is a projection of the magnetic field $\mathbf{B} \in \mathbf{H}_0^h(\text{div})$ to avoid helicity pollution in discretization. This auxiliary variable is exactly that indicated by the framework of [2]. We then consider the following discretization:

PROBLEM 4.1 (projection-based scheme). *At time step $n \geq 0$, find*

$$(\mathbf{B}_h^{n+1}, \mathbf{u}_h^{n+1/2}, \mathbf{E}_h^{n+1/2}, \mathbf{j}_h^{n+1/2}, \mathbf{H}_h^{n+1/2}) \in [\mathbf{H}_0^h(\text{div})]^2 \times [\mathbf{H}_0^h(\text{curl})]^3$$

such that for all test functions $(\mathbf{C}_h, \mathbf{v}_h, \mathbf{F}_h, \mathbf{k}_h, \mathbf{D}_h) \in [\mathbf{H}_0^h(\text{div})]^2 \times [\mathbf{H}_0^h(\text{curl})]^3$,

$$(4.2a) \quad \left(\frac{\mathbf{B}_h^{n+1} - \mathbf{B}_h^n}{\Delta t}, \mathbf{C}_h \right) + (\nabla \times \mathbf{E}_h^{n+1/2}, \mathbf{C}_h) = 0,$$

$$(4.2b) \quad (\mathbf{E}_h^{n+1/2}, \mathbf{F}_h) + (\mathbf{u}_h^{n+1/2} \times \mathbf{H}_h^{n+1/2}, \mathbf{F}_h) = 0,$$

$$(4.2c) \quad (\mathbf{j}_h^{n+1/2}, \mathbf{k}_h) - (\mathbf{B}_h^{n+1/2}, \nabla \times \mathbf{k}_h) = 0,$$

$$(4.2d) \quad (\mathbf{u}_h^{n+1/2}, \mathbf{v}_h) - \tau (\mathbf{j}_h^{n+1/2} \times \mathbf{H}_h^{n+1/2}, \mathbf{v}_h) = 0,$$

$$(4.2e) \quad (\mathbf{H}_h^{n+1/2}, \mathbf{D}_h) - (\mathbf{B}_h^{n+1/2}, \mathbf{D}_h) = 0.$$

The time discretization strategy is the same as that of Section 3; the difference is the introduction of the auxiliary variable. For the solver, we apply Newton iteration and solve the linearized system by the direct solver MUMPS [1]. The introduction of $\mathbf{H}_h^{n+1/2}$ that computes the projection of the magnetic field $\mathbf{B}_h^{n+1/2}$ from $\mathbf{H}_0^h(\text{div})$ to $\mathbf{H}_0^h(\text{curl})$ leads to helicity structure-preservation:

THEOREM 4.2. *Assume $(\mathbf{B}_h^{n+1}, \mathbf{u}_h^{n+1/2}, \mathbf{E}_h^{n+1/2}, \mathbf{j}_h^{n+1/2}, \mathbf{H}_h^{n+1/2})$ is a solution of (4.2). Then the energy is nonincreasing and the discrete Gauss law holds. Moreover, the (global) discrete Arnold inequality holds*

$$(4.3) \quad |\mathcal{H}_h^n| \leq C \mathcal{E}_h^n, \quad n \geq 0,$$

where $\mathcal{H}_h^{n+1} = (\mathbf{A}_h^n, \mathbf{B}_h^n)$, and the local helicity is conserved in the sense that

$$(4.4) \quad \int_{\Omega_{s,h}} \mathbf{B}_h^{n+1} \cdot \mathbf{A}_h^{n+1} \, dx = \int_{\Omega_{s,h}} \mathbf{B}_h^n \cdot \mathbf{A}_h^n \, dx = \dots = \int_{\Omega_{s,h}} \mathbf{B}_h^0 \cdot \mathbf{A}_h^0 \, dx,$$

where $\Omega_{s,h} \subset \Omega_h$ is any discrete magnetically closed subdomain such that for any $n \geq 0$ it holds that $\mathbf{B}_h^n \in \mathbf{H}_0^h(\text{div}, \Omega_{s,h})$.

Proof. The proof of the energy decay, the discrete Gauss law and the discrete Arnold inequality can be found in [28]. For the preservation of local helicity, we first notice that by definition there exists a vector potential

$$(4.5) \quad \mathbf{A}_h^{n+1/2} = \frac{\mathbf{A}_h^{n+1} + \mathbf{A}_h^n}{2} \in \mathbf{H}_0^h(\text{curl}, \Omega_{s,h}), \quad \nabla \times \mathbf{A}_h^{n+1/2} = \mathbf{B}_h^{n+1/2}.$$

Therefore, by taking $\mathbf{C}_h = \mathbf{A}_h^{n+1/2} \in \mathbf{H}_0^h(\text{curl}, \Omega_{s,h})$, we get (see [29, Theorem 5] for a similar argument)

$$\begin{aligned} & \int_{\Omega_{s,h}} \mathbf{B}_h^{n+1} \cdot \mathbf{A}_h^{n+1} \, dx - \int_{\Omega_{s,h}} \mathbf{B}_h^n \cdot \mathbf{A}_h^n \, dx \\ &= \int_{\Omega_{s,h}} (\mathbf{B}_h^{n+1} - \mathbf{B}_h^n) \cdot \mathbf{A}_h^{n+1/2} \, dx + \int_{\Omega_{s,h}} (\mathbf{A}_h^{n+1} - \mathbf{A}_h^n) \cdot \mathbf{B}_h^{n+1/2} \, dx \\ &= 2 \int_{\Omega_{s,h}} (\mathbf{B}_h^{n+1} - \mathbf{B}_h^n) \cdot \mathbf{A}_h^{n+1/2} \, dx = -2\Delta t \int_{\Omega_{s,h}} \mathbf{E}_h^{n+1/2} \cdot \mathbf{B}_h^{n+1/2} \, dx, \end{aligned}$$

the proof is then complete by noting that from (4.2b) and (4.2e), we have

$$(4.6) \quad \mathbf{E}_h^{n+1/2} = -\mathbb{Q}_h^{\text{curl}}(\mathbf{u}_h^{n+1/2} \times \mathbb{Q}_h^{\text{curl}} \mathbf{B}_h^{n+1/2}),$$

where $\mathbb{Q}_h^{\text{curl}}$ is the L^2 projection operator. \square

REMARK 4.3. *The discrete Arnold inequality can be proven for any magnetic closed subdomain, i.e.*

$$(4.7) \quad \left| \int_{\Omega_{s,h}} \mathbf{B}_h^n \cdot \mathbf{A}_h^n \, dx \right| \leq C \int_{\Omega_{s,h}} \mathbf{B}_h^n \cdot \mathbf{B}_h^n \, dx.$$

Without qualification, by the Arnold inequality we mean the global version, i.e., the above inequality with $\Omega_{s,h} = \Omega$.

5. The Lagrange multiplier scheme. In this part, we introduce a scheme that preserves the global helicity by using a Lagrange multiplier. This approach is inspired by a family of structure-preserving methods for gradient systems [13,14], the Klein–Gordon–Schrödinger system [26], the geometric evolution equation [23], a two-phase Stokes model [24], and incompressible flows based on finite element exterior calculus [46]. The key idea is to incorporate scalar variables with energy/helicity variational terms and the evolution equation will reduce to continuous model under mild conditions. Here the evolution equation can either be chosen for the magnetic field \mathbf{B} (4.1a) or the magnetic potential \mathbf{A} (5.1). We choose the latter since it will lead to a discrete scheme that does not violate the discrete Arnold inequality (see Theorem 5.4 below).

We therefore reformulate (4.1a) in terms of the magnetic potential \mathbf{A} :

$$(5.1) \quad \partial_t \mathbf{A} + \mathbf{E} = \mathbf{0}.$$

The energy and helicity can be rewritten in terms of \mathbf{A} as

$$(5.2) \quad \mathcal{E} = \mathcal{E}(\mathbf{A}) = (\nabla \times \mathbf{A}, \nabla \times \mathbf{A}), \quad \mathcal{H} = \mathcal{H}(\mathbf{A}) = (\nabla \times \mathbf{A}, \mathbf{A}).$$

5.1. Model derivation. We introduce two Lagrange multipliers into (5.1) to enforce the energy law and helicity conservation. This yields the following evolution equation

$$(5.3) \quad \partial_t \mathbf{A} + \mathbf{E} + \lambda_\varepsilon \frac{\delta \mathcal{E}}{\delta \mathbf{A}} + \lambda_{\mathcal{H}} \frac{\delta \mathcal{H}}{\delta \mathbf{A}} = \mathbf{0}.$$

Using Woltjer's variational principle (see Appendix A) [49], we have

$$(5.4) \quad \frac{\delta \mathcal{E}}{\delta \mathbf{A}} = 2\mathbf{j}, \quad \frac{\delta \mathcal{H}}{\delta \mathbf{A}} = 2\mathbf{B},$$

where $\mathbf{j} = \nabla \times \mathbf{B} = \nabla \times \nabla \times \mathbf{A}$.

This leads to the continuous PDE system with variables $(\mathbf{B}, \mathbf{u}, \mathbf{A}, \mathbf{E}, \mathbf{j}, \lambda_\varepsilon, \lambda_{\mathcal{H}})$

$$(5.5a) \quad \partial_t \mathbf{A} + \mathbf{E} + \lambda_{\mathcal{H}} \mathbf{B} + \lambda_\varepsilon \mathbf{j} = \mathbf{0},$$

$$(5.5b) \quad \mathbf{B} = \nabla \times \mathbf{A},$$

$$(5.5c) \quad \mathbf{u} - \tau \mathbf{j} \times \mathbf{B} = \mathbf{0},$$

$$(5.5d) \quad \mathbf{E} + \mathbf{u} \times \mathbf{B} = \mathbf{0},$$

$$(5.5e) \quad \mathbf{j} = \nabla \times \mathbf{B},$$

$$(5.5f) \quad \frac{d}{dt} \mathcal{E} = -2\tau \|\mathbf{j} \times \mathbf{B}\|^2,$$

$$(5.5g) \quad \frac{d}{dt} \mathcal{H} = 0.$$

The last two scalar equations enforce the energy law and helicity conservation. The Lagrange multipliers reduce to zero under mild conditions and this model is equivalent to (1.1) and (4.1).

THEOREM 5.1. *Assume $(\mathbf{B}, \mathbf{u}, \mathbf{A}, \mathbf{E}, \mathbf{j})$ and $(\lambda_\varepsilon, \lambda_{\mathcal{H}})$ are the solution of system (5.5). Then $\lambda_\varepsilon = \lambda_{\mathcal{H}} = 0$ if $\mathbf{j} \times \mathbf{B} \neq \mathbf{0}$.*

Proof. Testing the evolution equation (5.5a) with \mathbf{j} , we obtain

$$0 = (\partial_t \mathbf{A}, \mathbf{j}) + (\mathbf{E}, \mathbf{j}) + \lambda_\varepsilon \|\mathbf{j}\|^2 + \lambda_{\mathcal{H}} (\mathbf{B}, \mathbf{j}).$$

With (5.5b)–(5.5f) and straightforward computation, the first two terms give

$$\begin{aligned} (\partial_t \mathbf{A}, \mathbf{j}) + (\mathbf{E}, \mathbf{j}) &= (\partial_t \mathbf{A}, \nabla \times \mathbf{B}) - (\mathbf{u} \times \mathbf{B}, \mathbf{j}) \\ &= (\partial_t \mathbf{B}, \mathbf{B}) + \tau \|\mathbf{j} \times \mathbf{B}\|^2 \\ &= \frac{1}{2} \left(\frac{d}{dt} \mathcal{E} + 2\tau \|\mathbf{j} \times \mathbf{B}\|^2 \right) = 0, \end{aligned}$$

where in the last line we used the enforced energy law. Thus we have

$$(5.6) \quad \lambda_\varepsilon \|\mathbf{j}\|^2 + \lambda_{\mathcal{H}} (\mathbf{B}, \mathbf{j}) = 0.$$

On the other hand, testing (5.5a) with \mathbf{B} , we obtain

$$0 = (\partial_t \mathbf{A}, \mathbf{B}) + (\mathbf{E}, \mathbf{B}) + \lambda_\varepsilon (\mathbf{j}, \mathbf{B}) + \lambda_{\mathcal{H}} \|\mathbf{B}\|^2.$$

Then using (5.5b), (5.5d) and (5.5g), we get

$$(\partial_t \mathbf{A}, \mathbf{B}) + (\mathbf{E}, \mathbf{B}) = \frac{1}{2} \frac{d\mathcal{H}}{dt} = 0.$$

Therefore, we derive another equation for Lagrange multipliers

$$(5.7) \quad \lambda_{\mathcal{E}}(\mathbf{j}, \mathbf{B})^2 + \lambda_{\mathcal{H}}\|\mathbf{B}\|^2 = 0.$$

To summarize, the two Lagrange multipliers satisfy

$$(5.8) \quad \begin{pmatrix} \|\mathbf{B}\|^2 & (\mathbf{j}, \mathbf{B}) \\ (\mathbf{j}, \mathbf{B}) & \|\mathbf{j}\|^2 \end{pmatrix} \begin{pmatrix} \lambda_{\mathcal{H}} \\ \lambda_{\mathcal{E}} \end{pmatrix} = \begin{pmatrix} 0 \\ 0 \end{pmatrix}.$$

Thus, the determinant of the matrix is

$$(5.9) \quad \|\mathbf{B}\|^2\|\mathbf{j}\|^2 - (\mathbf{j}, \mathbf{B})^2 > 0,$$

if $\mathbf{B} \not\parallel \mathbf{j}$, i.e. $\mathbf{j} \times \mathbf{B} \neq \mathbf{0}$. In this case, the Lagrange multipliers vanish. \square

COROLLARY 5.2. *Assume the solution to (5.1) is continuous in time. Then the magneto-friction equation (1.1) is equivalent to (5.5) in the sense that any solutions to (5.1) combined with $\lambda_{\mathcal{E}} = \lambda_{\mathcal{H}} = 0$ solves (5.5), and any solutions to (5.5) satisfy $\lambda_{\mathcal{E}} = \lambda_{\mathcal{H}} = 0$ and thus solves (1.1).*

Proof. **Theorem 5.1** implies that before reaching a stationary state, the Lagrange multipliers in (5.5) vanish. Thus the solutions to the two systems are equivalent. Since the solutions are assumed to be continuous in time, this equivalence also extends to stationary states. \square

5.2. Full discretization. We discretize (5.5) using finite element exterior calculus in space and implicit Euler time stepping.

PROBLEM 5.3 (Lagrange multiplier scheme). *For each time step $n \geq 0$, we find*

$$(\mathbf{B}_h^{n+1}, \mathbf{u}_h^{n+1}, \mathbf{A}_h^{n+1}, \mathbf{E}_h^{n+1}, \mathbf{j}_h^{n+1}) \in [\mathbf{H}_0^h(\text{div})]^2 \times [\mathbf{H}_0^h(\text{curl})]^3$$

and $(\lambda_{\mathcal{E},h}^{n+1}, \lambda_{\mathcal{H},h}^{n+1}) \in \mathbb{R}^2$ such that for $(\mathbf{C}_h, \mathbf{v}_h, \mathbf{D}_h, \mathbf{F}_h, \mathbf{k}_h) \in [\mathbf{H}_0^h(\text{div})]^2 \times [\mathbf{H}_0^h(\text{curl})]^3$,

$$(5.10a) \quad \begin{aligned} & \left(\frac{\mathbf{A}_h^{n+1} - \mathbf{A}_h^n}{\Delta t}, \mathbf{D}_h \right) + (\mathbf{E}_h^{n+1}, \mathbf{D}_h) \\ & + \lambda_{\mathcal{H},h}^{n+1}(\mathbf{B}_h^{n+1}, \mathbf{D}_h) + \lambda_{\mathcal{E},h}^{n+1}(\mathbf{j}_h^{n+1}, \mathbf{D}_h) = 0, \end{aligned}$$

$$(5.10b) \quad (\mathbf{B}_h^{n+1}, \mathbf{C}_h) - (\nabla \times \mathbf{A}_h^{n+1}, \mathbf{C}_h) = 0,$$

$$(5.10c) \quad (\mathbf{u}_h^{n+1}, \mathbf{v}_h) - \tau(\mathbf{j}_h^{n+1} \times \mathbf{B}_h^{n+1}, \mathbf{v}_h) = 0,$$

$$(5.10d) \quad (\mathbf{E}_h^{n+1}, \mathbf{F}_h) + (\mathbf{u}_h^{n+1} \times \mathbf{B}_h^{n+1}, \mathbf{F}_h) = 0,$$

$$(5.10e) \quad (\mathbf{j}_h^{n+1}, \mathbf{k}_h) - (\mathbf{B}_h^{n+1}, \nabla \times \mathbf{k}_h) = 0,$$

$$(5.10f) \quad \frac{\mathcal{E}_h^{n+1} - \mathcal{E}_h^n}{\Delta t} + 2\tau\|\mathbf{B}_h^{n+1} \times \mathbf{j}_h^{n+1}\|^2 = 0,$$

$$(5.10g) \quad \mathcal{H}_h^{n+1} - \mathcal{H}_h^n = 0.$$

THEOREM 5.4. *Let $(\mathbf{B}_h^{n+1}, \mathbf{u}_h^{n+1}, \mathbf{A}_h^{n+1}, \mathbf{E}_h^{n+1}, \mathbf{j}_h^{n+1})$ and $(\lambda_{\mathcal{E},h}^{n+1}, \lambda_{\mathcal{H},h}^{n+1})$ be a solution of (5.10). The energy law (3.2) and the discrete Gauss law hold. Moreover, the global helicity is conserved:*

$$(5.11) \quad \mathcal{H}_h^{n+1} = \mathcal{H}_h^n = \dots = \mathcal{H}_h^0, \quad n \geq 0,$$

and the discrete Arnold's inequality holds.

Proof. The energy-decreasing and the helicity-preserving properties are direct consequences of (5.10f) and (5.10g) respectively. Moreover, from (5.10b), we have

$$\mathbf{B}_h^{n+1} = \nabla \times \mathbf{A}_h^{n+1}.$$

Taking the divergence, we get $\nabla \cdot \mathbf{B}_h^{n+1} = 0$. Finally, the discrete Arnold inequality follows from (5.10b) and the discrete Poincaré inequality

$$\begin{aligned} |\mathcal{H}_h^{n+1}| &= |(\mathbf{A}_h^{n+1}, \mathbf{B}_h^{n+1})| \leq \|\mathbf{A}_h^{n+1}\| \|\mathbf{B}_h^{n+1}\| \\ &\leq C \|\nabla \times \mathbf{A}_h^{n+1}\| \|\mathbf{B}_h^{n+1}\| \\ &\leq C \|\mathbf{B}_h^{n+1}\|^2 = C \mathcal{E}_h^{n+1}, \end{aligned}$$

where C is a positive constant independent of n . \square

REMARK 5.5. *The condition $\mathbf{j} \times \mathbf{B} = \mathbf{0}$ leads the degeneracy of the matrix (5.8), which also makes the Lagrange multiplier scheme (5.10) difficult to converge when reaching the steady state. The Lagrange multiplier approach must be modified so that the scheme can support long-time evolution [13, 14, 23, 24]. If $\Delta \mathcal{E}_h^{n+1} = \frac{\mathcal{E}_h^{n+1} - \mathcal{E}_h^n}{\Delta t} < \gamma$, where $\gamma \ll 1$ we continue with the Lagrange multiplier method as presented. Otherwise, we set $\lambda_\mathcal{E} = 0$ and omit (5.10f), and only preserve global helicity. In the subsequent numerical experiments, we always set $\gamma = 9 \times 10^{-5}$.*

5.3. Solver. For each time step, we apply Newton linearization for the coupled system (5.10). The linearized Newton system for the unknowns

$$(5.12) \quad (\mathbf{B}_h^{n+1}, \mathbf{u}_h^{n+1}, \mathbf{A}_h^{n+1}, \mathbf{E}_h^{n+1}, \mathbf{j}_h^{n+1}, \lambda_{\mathcal{E},h}^{n+1}, \lambda_{\mathcal{H},h}^{n+1})$$

naturally has a saddle point structure due to the presence of the Lagrange multipliers. We group the degrees of freedom into a vector of *physical fields*,

$$(5.13) \quad x_f = (\mathbf{B}, \mathbf{u}, \mathbf{A}, \mathbf{E}, \mathbf{j}),$$

and a vector of *Lagrange multipliers*,

$$(5.14) \quad x_\lambda = (\lambda_\mathcal{E}, \lambda_\mathcal{H}),$$

which yields a 2×2 block system

$$(5.15) \quad \begin{pmatrix} A & B \\ C & 0 \end{pmatrix} \begin{pmatrix} x_f \\ x_\lambda \end{pmatrix} = \begin{pmatrix} f_f \\ f_\lambda \end{pmatrix}.$$

The right hand side functions f_f and f_λ are the residual in the Newton iterations. We solve (5.15) with a block preconditioner. We first use flexible GMRES [43] as the outermost solver. We then split the physical fields from the Lagrange multipliers. More precisely, we use the full block factorization preconditioner [32, 39]

$$(5.16) \quad \mathcal{P}^{-1} = \begin{pmatrix} I & 0 \\ CA^{-1} & I \end{pmatrix} \begin{pmatrix} A & 0 \\ 0 & S \end{pmatrix} \begin{pmatrix} I & A^{-1}B \\ 0 & I \end{pmatrix},$$

where $S = -CA^{-1}B$ is the Schur complement. The physical block is then solved by a direct solver; we employ MUMPS [1]. The Schur complement involves only two scalar multipliers. A GMRES with a maximum 2 iterations is applied, which is sufficient in exact arithmetic. All operations are performed in a matrix-free way, except for the direct solve of A . The above solver is implemented using PETSc's built-in Schur complement infrastructure [8].

6. Numerical experiments. We simulate magnetic relaxation with two magnetic configurations, the E^3 -field (magnetic braids) and the Hopf fibration (magnetic knots). We do using the three schemes considered: the non-conservative scheme (3.1) that preserves no helicity constraint, the projection-based scheme (4.2) with local helicity constraints, and the Lagrange multiplier method (5.10) with the global helicity constraint. We monitor the evolution of the energy and helicity.

The computational domain is chosen to be a cuboid

$$(6.1) \quad \Omega = (-4, 4)^2 \times (-Z, Z),$$

where $Z = 10$ for the Hopf fibration and $Z = 24$ for the E^3 -field. Closed boundary conditions (2.4) are imposed on all faces. The helicity is well-defined under magnetically closed boundary conditions $\mathbf{B} \cdot \mathbf{n} = 0$. For the E^3 -field, the background field $\mathbf{B}_0 \mathbf{e}_z$ corresponds to the harmonic form, which has been shown to be constant [28, Theorem 3.4]. Therefore, we first subtract this harmonic component, perform the computation, and then add it back for visualization purposes.

The coupling parameter is fixed at $\tau = 1$. Unless stated otherwise, we employ a coarse mesh consisting of $4 \times 4 \times 10$ hexahedral cells for the Hopf fibration and $4 \times 4 \times 24$ hexahedral cells for the E^3 -field in the $x \times y \times z$ directions. For spatial discretization, we use, in each case, the lowest-order Nédélec edge and face elements of the first kind belonging to the same de Rham complex. These under-resolved discretizations stress-test the structure-preserving properties of the algorithms.

REMARK 6.1. *In the present work, we have fixed the boundary conditions to be magnetically closed and for brevity do not address their influence on the equilibrium structure. Though theoretical existence of equilibria is open for MF, numerical evidence [41, 50] show that the choice of boundary conditions (line-tied, periodic and closed) can fundamentally alter the nature of braided equilibria. We leave a systematic investigation of this dependence to future work.*

6.1. Magnetic braids: E^3 -field. We first consider magnetic braids: the E^3 -field [12, 41], which is constructed by concatenating three identical elementary units, each consisting of one positive and one negative twist superimposed on a uniform background field. Therefore, the global helicity vanishes by construction. Note that Arnold's inequality does not guarantee a topological barrier for the E^3 -field and thus a physically faithful simulation is even more challenging (than initial fields with non-zero helicity). The initial magnetic configuration is

$$(6.2) \quad \mathbf{B}^{E^3}(0) = B_0 \mathbf{e}_z + \sum_{c=1}^6 \frac{2kB_0}{a} (-(y - y_c) \mathbf{e}_x + (x - x_c) \mathbf{e}_y) \times \exp \left[-\frac{(x - x_c)^2}{a^2} - \frac{(y - y_c)^2}{a^2} - \frac{(z - z_c)^2}{l^2} \right],$$

with the initial field strength B_0 , strength of twist k , radius and length in the z -direction of the twist region a and l , respectively. The twist locations are (x_c, y_c, z_c) . We choose $x_c = \{1, -1, 1, -1, 1, -1\}$, $y_c = \{0, \dots, 0\}$, $z_c = \{-20, -12, -4, 4, 12, 20\}$, and $a = \sqrt{2}, l = 2, B_0 = 1, k = 5$. For the time stepping, we choose $\Delta t = 0.1$ and $\tau = 1$ at the beginning of 100 time steps and then change to a larger time step $\Delta t = 100$ and $\tau = 0.1$ to accelerate our relaxation.

Figures 6.1 and 6.2 illustrate the evolution of the energy and helicity and magnetic line distribution of the E^3 -field for the different schemes. During the relaxation process, magnetic reconnections occur in both the non-conservative scheme and the

Lagrange multiplier method, causing the braided structures to gradually untangle and the magnetic field to relax toward an unknotted, rectilinear configuration; both schemes therefore converge to a trivial minimum with complete dissipation of magnetic energy. By contrast, the projection-based scheme produces an equilibrium that preserves complex local topology, leading to a non-trivial steady state with strictly positive magnetic energy.

As a partial conclusion, the Lagrange multiplier scheme only enforces the global helicity constraint and therefore fails to reach a nontrivial steady state when starting from the E^3 -field configuration. In contrast, the projection-based scheme preserves local helicity conservation and evolves toward a nontrivial equilibrium that retains complex local topology.

REMARK 6.2. *It remains open to rigorously prove that the projection-based method leads to a nontrivial steady state for the E^3 -initial configuration. Similar argument as in [28] fails since the global helicity vanishes and the Arnold inequality does not provide a guarantee of a lower bound of energy. On the continuous level, one can show that with some technical assumptions, any topologically nontrivial initial configurations evolve to nontrivial steady states [22]. However, establishing a discrete version of this result is beyond the scope of this paper.*

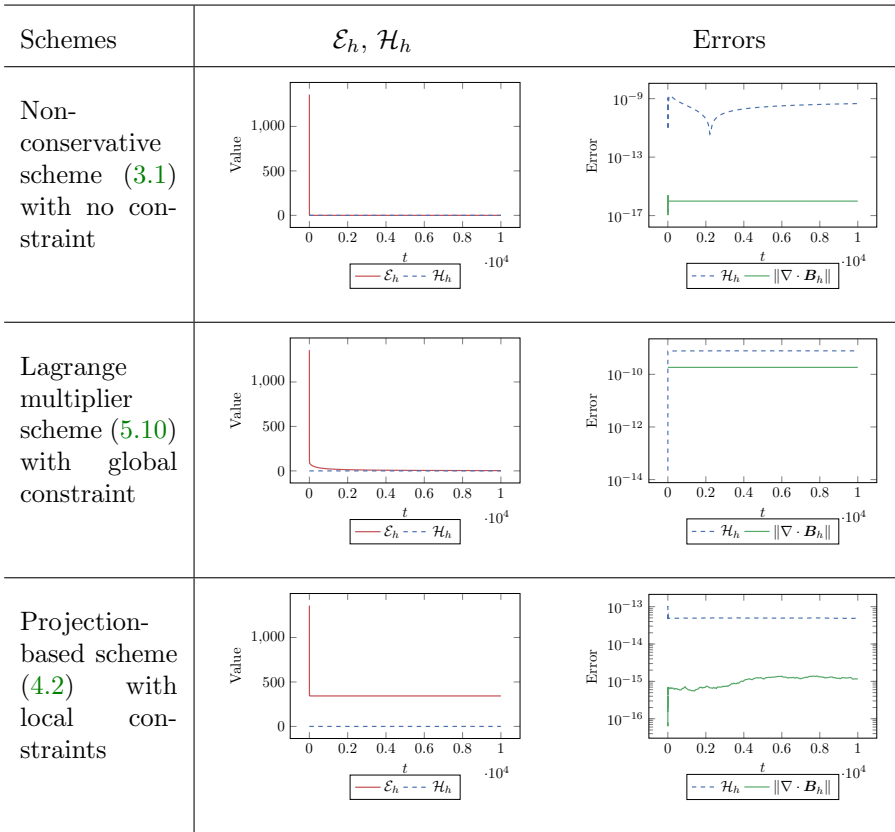


Fig. 6.1: Magnetic braids (E^3 -field): evolution of energy and helicity, errors.

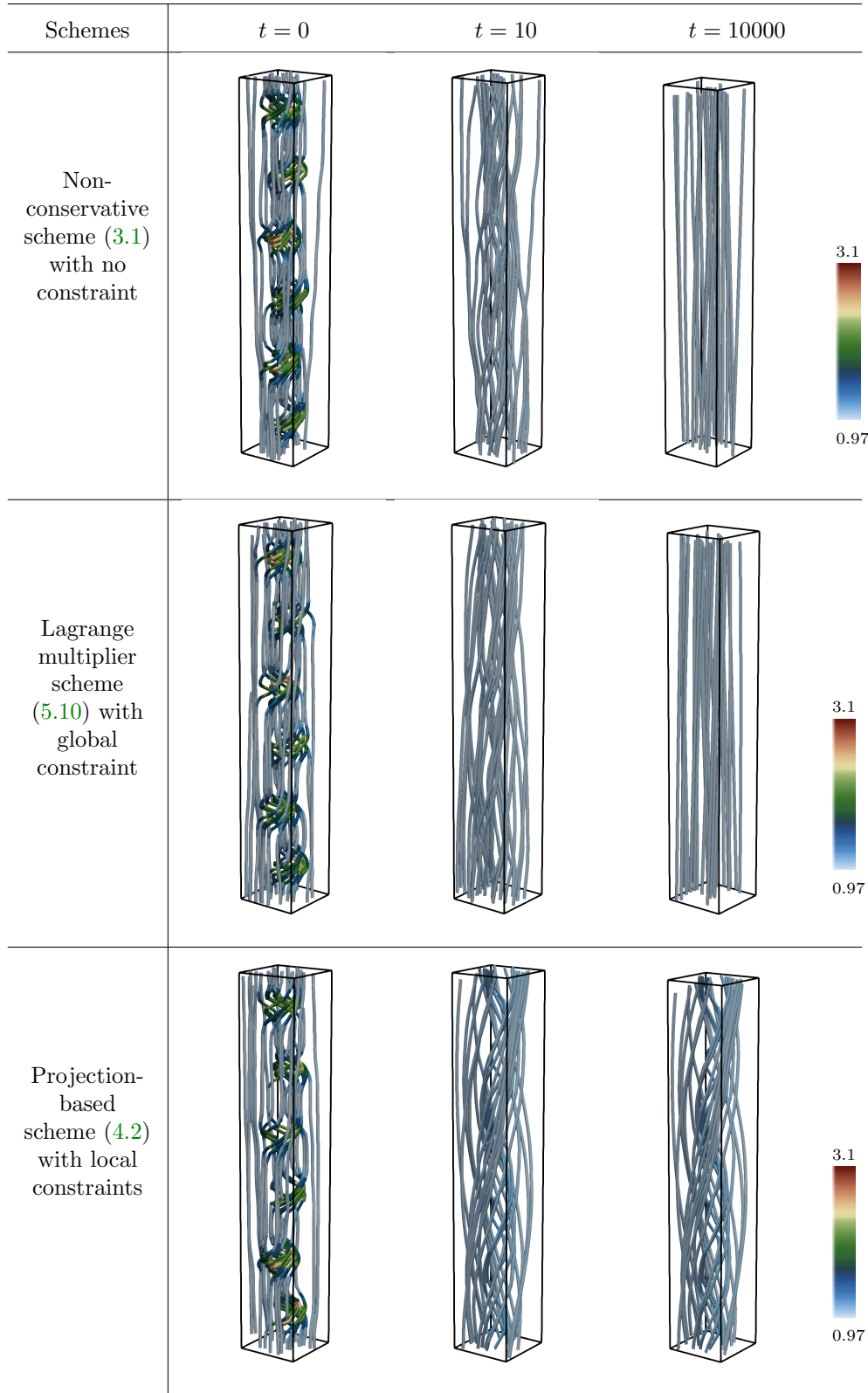


Fig. 6.2: *Magnetic braids*: comparison of evolution of stream tubes of the magnetic field under different topological constraints, colored by magnetic field strength $\|B_h\|$.

6.2. Magnetic knots: Hopf fibration. We next consider the relaxation of magnetic knots, employing the Hopf fibration as the initial configuration [44]

$$(6.3) \quad \mathbf{B}^{\text{Hopf}}(0) = \frac{4\sqrt{s}}{\pi(1+r^2)^3\sqrt{\omega_1^2+\omega_2^2}} \begin{pmatrix} 2(\omega_2 y - \omega_1 x z) \\ -2(\omega_2 x + \omega_1 y z) \\ \omega_1(-1+x^2+y^2-z^2) \end{pmatrix},$$

where $\omega_1, \omega_2 \in \mathbb{R}$ are winding numbers, $s \geq 0$ is a scaling parameter, and $r^2 = x^2 + y^2 + z^2$. We choose $\omega_1 = 3$, $\omega_2 = 2$, $s = 1$, such that the field lines form three windings in the poloidal direction for every two in the toroidal direction, thus exhibiting a non-zero helicity. For the time stepping, we choose $\Delta t = 1$ and $\tau = 1$ at the beginning of 100 time steps and then change to a larger time step $\Delta t = 100$ and $\tau = 0.1$ to accelerate our relaxation.

Figure 6.4 presents snapshots of the relaxation process with the three schemes. The equilibria reached at $t = 10000$ clearly exhibit distinct morphological features depending on the constraints enforced. This qualitative difference is further quantified by the time evolution of key physical quantities shown in Figure 6.3.

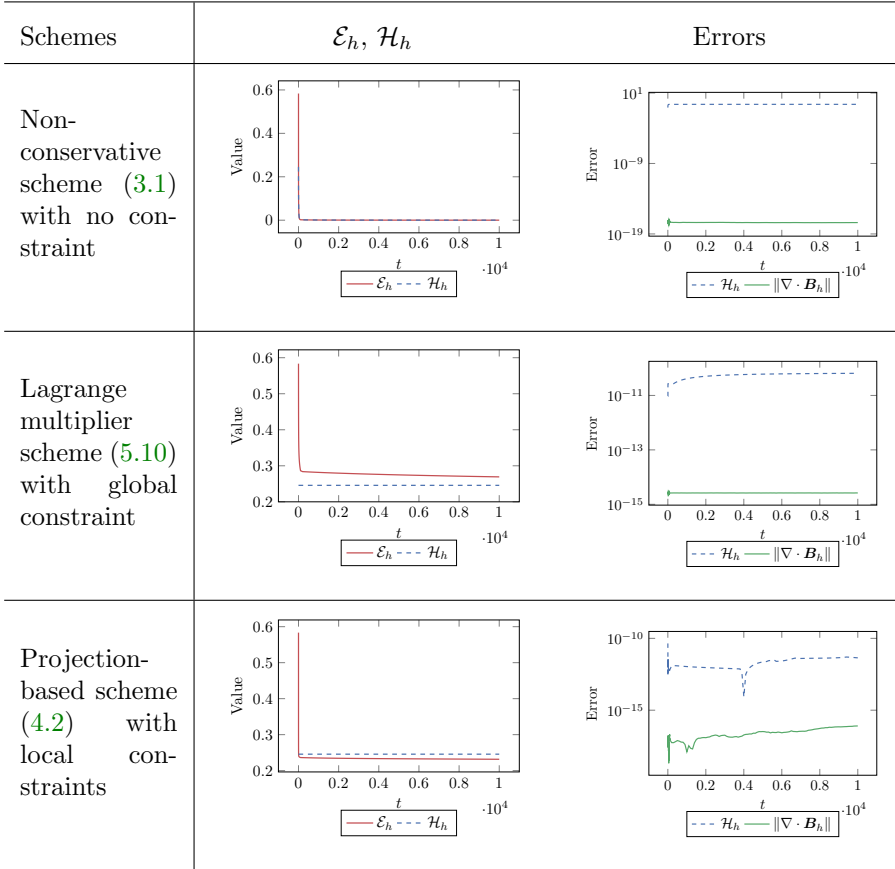


Fig. 6.3: Magnetic knots (Hopf fibration): evolution of energy and helicity, errors.

Based on these numerical results, several conclusions can be drawn. In the absence of the discrete Arnold inequality, the non-conservative scheme permits the magnetic

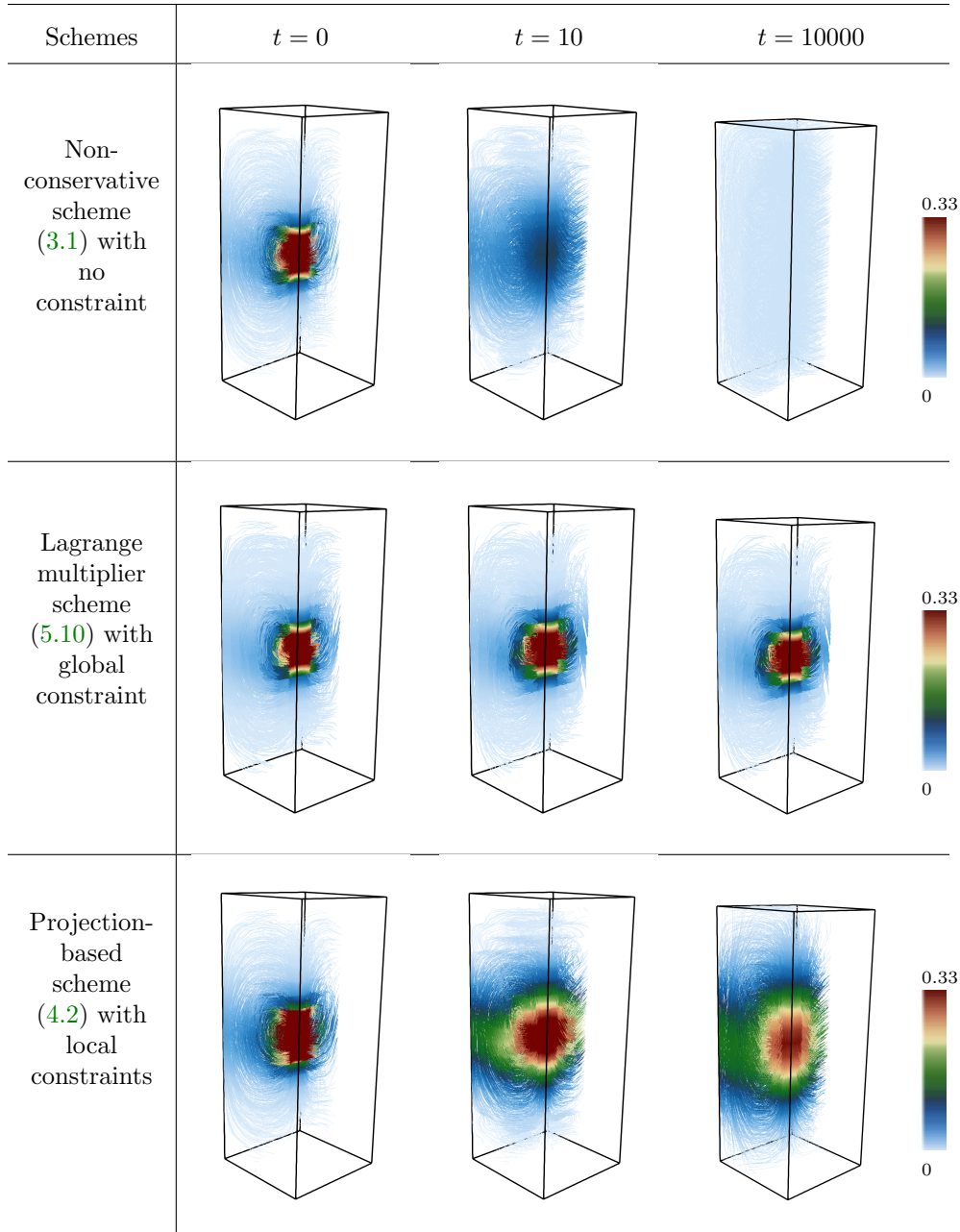


Fig. 6.4: *Magnetic knots*: comparison of evolution of stream tubes of the magnetic field under different topological constraints, colored by magnetic field strength $\|\mathcal{B}_h\|$.

energy to decay to (or very near) zero, confirming that without explicit topological protection, the magnetic field relaxes to a trivial state. Both the Lagrange multiplier and projection-based schemes, by contrast, converge to steady states with distinctly non-zero energy levels, consistent with Arnold's inequality, which asserts that non-

trivial topology imposes a lower bound on the minimizable magnetic energy. The non-conservative scheme preserves only the discrete Gauss law, whereas both the Lagrange multiplier and projection-based schemes maintain the discrete Gauss law *and* global magnetic helicity to within machine precision and solver tolerances, thereby preserving the topological integrity of the field throughout the evolution.

Strikingly, the Lagrange multiplier scheme (5.10) and the projection-based scheme (4.2) produce different steady states. Although both formulations are derived for the same PDE, the projection-based scheme more faithfully preserves at the discrete level the set of physical invariants and is therefore more reliable. Nevertheless, the nontrivial equilibrium obtained with the Lagrange multiplier scheme appears more physically relevant, as will be explained in the following section.

7. Local vs. global helicity preservation: physical implications. We have examined two helicity-preserving schemes for the magneto-frictional equations: one based on projection with auxiliary variables and the other based on a Lagrange multiplier approach. These schemes respectively enforce all local helicity constraints and a single global helicity constraint at the discrete level. The different steady states produced by these two methods raise a natural question: given that the projection-based scheme preserves *all* local helicities in ideal MHD and magneto-friction, does the weaker Lagrange multiplier approach remain relevant?

We believe it does. In reality, ideal MHD and its model problem (1.1) are only approximations of genuine plasma-physics systems, where diffusion of varying strengths and magnetic reconnection events occur during dynamical evolution. When diffusion and *local* reconnection are present, local helicities are no longer conserved, whereas global magnetic helicity remains conserved (at least approximately, and often to high accuracy) [41, 45]. A well-known example is Taylor relaxation, in which small-scale reconnection events are believed to progressively rearrange magnetic topology while preserving the total helicity, thereby driving the system toward a minimum-energy state consistent with this single global invariant. This physical picture, originally proposed by Taylor, has proven remarkably successful: theoretical predictions closely match experimental observations in reverse-field pinches [45].

In this context, our numerical experiments with the E^3 -field (see Figure 6.2) demonstrate that the Lagrange multiplier method naturally permits such local reconnection events and allows corresponding changes in field-line topology. This behavior qualitatively reproduces a key feature of real plasma relaxation phenomena. In this context, the ideal equations overly constrain the dynamics and suppress these physically important local processes.

Solving the ideal MHD or the magneto-frictional equations with the “wrong” (i.e., merely global-helicity-conserving) scheme may, in fact, be closer to the real physics than the idealized equations themselves suggest. Numerical errors (relative to the true solutions of the ideal MHD or magneto-friction equations) arise from the weaker enforcement of the helicity constraint at local scales. Rather than viewing these deviations purely as undesirable artifacts, one can interpret them as mimicking physical local reconnection processes while still preserving helicity in a global, averaged sense.

This naturally raises the question: Can schemes based on the Lagrange multiplier approach be used to study Taylor relaxation and related phenomena? More broadly, can controlled numerical violations at small scales serve as a meaningful surrogate for unresolved physical reconnection processes, while preserving the correct global invariants? In short, the key issue is *whether solving the ideal MHD equations with such “incorrect” algorithms can, in practice, yield physically more realistic solutions.*

In this work we do not provide a definitive answer. Instead, we view these results as opening a promising direction for further investigation. We also note that Faraco et al. [20] recently proposed a helicity conservation condition designed to better match the real physics of Taylor relaxation. Inspired by this and related work, a deeper understanding of the interplay between numerical constraint enforcement, topological evolution, and physical reconnection processes may yield new insights into relaxation theory and guide the design of structure-preserving numerical schemes for magnetohydrodynamics.

8. Conclusion. In this work, we have investigated magnetic relaxation under three distinct levels of topological constraint: unconstrained evolution, global helicity conservation, and local helicity conservation. By systematically comparing three finite element discretizations that enforce these constraints at the discrete level, we have demonstrated that the degree to which helicity is preserved numerically plays a decisive role in determining the character of the relaxed magnetic state.

Numerical experiments with braided and knotted magnetic fields confirm that the three schemes converge to qualitatively distinct equilibria. In particular, we have shown that the Lagrange multiplier scheme alone is insufficient to obtain a nontrivial steady state from strongly braided initial configurations. Recall that the Arnold inequality provides no additional lower bound in such cases, as the initial data has vanishing helicity. Therefore, it is a nontrivial fact that the projection-based approach still evolves to nontrivial steady states with this initial magnetic field. This is justified only by numerical results, not by rigorous proofs; on the other hand, theoretical guarantees of the evolution of a broad class of topologically nontrivial fields can be found on the continuous level [22]. This observation also motivates the exploration of higher-order topological invariants, such as those conjectured in [7].

This raises an intriguing question: might the Lagrange multiplier approach better capture the essential physics of Taylor relaxation? This in turn raises a question on the best use of structure preservation in numerical PDEs: in real physical systems, which invariants should be rigidly preserved, and which may, or even should, be allowed to evolve or break on discretization?

Looking ahead, we plan to pursue several directions. Algorithmically, we intend to develop efficient solvers for all three methods, including the application of decoupling techniques and tailored preconditioners. From the physics perspective, we aim to apply these numerical schemes to study magnetic braids in the context of solar coronal heating [12, 41].

Code availability. The simulations in Section 6 were implemented in Firedrake [27] and PETSc [8]; MUMPS [1] was used to solve the linear systems. The code used to generate the numerical results and all Firedrake components have been archived on Zenodo [21].

Acknowledgments. We would like to thank Ralf Hiptmair, Gunnar Hornig, Anthony Yeates, and Simon Candelaresi for helpful discussions.

A. Woltjer’s variational principle. Following Woltjer [49], we solve the following variational problem subject to the global helicity \mathcal{H} , viewing both quantities as functions of \mathbf{A} ,

$$(A.1) \quad \frac{\delta}{\delta \mathbf{A}} (\mathcal{E} - \alpha_0 \mathcal{H}) = 0.$$

where α_0 is a Lagrange multiplier to enforce the global helicity conservation \mathcal{H} . Direct computation yields that

$$\begin{aligned} \frac{\delta \mathcal{E}}{\delta \mathbf{A}} &= 2 \int_{\Omega} \mathbf{B} \cdot \nabla \times \delta \mathbf{A} \, dx, \\ &= 2 \int_{\Omega} (\delta \mathbf{A} \cdot \nabla \times \mathbf{B} - \nabla \cdot [\mathbf{B} \times \delta \mathbf{A}]) \, dx, \\ &= 2 \int_{\Omega} \delta \mathbf{A} \cdot \mathbf{j} \, dx - 2 \int_{\partial \Omega} \mathbf{B} \cdot (\delta \mathbf{A} \times \mathbf{n}) \, dx, \\ &= 2 \int_{\Omega} \delta \mathbf{A} \cdot \mathbf{j} \, dx. \end{aligned}$$

Then, we compute

$$\begin{aligned} \frac{\delta \mathcal{H}}{\delta \mathbf{A}} &= \int_{\Omega} \delta \mathbf{A} \cdot \mathbf{B} \, dx + \int_{\Omega} \mathbf{A} \cdot \delta \mathbf{B} \, dx \\ &= \int_{\Omega} \delta \mathbf{A} \cdot \mathbf{B} \, dx + \int_{\Omega} \mathbf{A} \cdot (\nabla \times \delta \mathbf{A}) \, dx \\ &= \int_{\Omega} \delta \mathbf{A} \cdot \mathbf{B} \, dx + \int_{\Omega} \delta \mathbf{A} \cdot (\nabla \times \mathbf{A}) \, dx \\ &\quad - \int_{\partial \Omega} \mathbf{n} \cdot (\mathbf{A} \times \delta \mathbf{A}) \, dx \\ &= 2 \int_{\Omega} \delta \mathbf{A} \cdot \mathbf{B} \, dx - \int_{\partial \Omega} \mathbf{A} \cdot (\delta \mathbf{A} \times \mathbf{n}) \, dx \\ &= 2 \int_{\Omega} \delta \mathbf{A} \cdot \mathbf{B} \, dx. \end{aligned}$$

The minimum-energy state must satisfy

$$(A.2) \quad \int_{\Omega} \delta \mathbf{A} \cdot (\mathbf{j} - \alpha_0 \mathbf{B}) \, dx = 0.$$

Therefore, we have $\mathbf{j} = \alpha_0 \mathbf{B}$, where α_0 is a constant.

REFERENCES

- [1] P. R. AMESTOY, I. S. DUFF, J. KOSTER, AND J.-Y. L'EXCELLENT, *A fully asynchronous multi-frontal solver using distributed dynamic scheduling*, SIAM Journal on Matrix Analysis and Applications, 23 (2001), pp. 15–41.
- [2] B. D. ANDREWS AND P. E. FARRELL, *Enforcing conservation laws and dissipation inequalities numerically via auxiliary variables*, SIAM Journal on Scientific Computing, 47 (2025).
- [3] D. ARNOLD, R. FALK, AND R. WINTHER, *Finite element exterior calculus: from Hodge theory to numerical stability*, Bulletin of the American Mathematical Society, 47 (2010), pp. 281–354.
- [4] D. N. ARNOLD, *Finite Element Exterior Calculus*, Society for Industrial and Applied Mathematics, Philadelphia, PA, 2018.
- [5] D. N. ARNOLD, R. S. FALK, AND R. WINTHER, *Finite element exterior calculus, homological techniques, and applications*, Acta Numerica, 15 (2006), pp. 1–155.
- [6] V. I. ARNOLD, *The asymptotic Hopf invariant and its applications*, Vladimir I. Arnold- Collected Works: Hydrodynamics, Bifurcation Theory, and Algebraic Geometry 1965-1972, (1974), pp. 357–375.
- [7] V. I. ARNOLD AND B. A. KHESIN, *Topological Methods in Hydrodynamics*, vol. 125 of Applied Mathematical Sciences, Springer International Publishing, Cham, 2021.
- [8] S. BALAY, S. ABHYANKAR, M. F. ADAMS, S. BENSON, J. BROWN, P. BRUNE, K. BUSCHELMAN, E. CONSTANTINESCU, L. DALCIN, A. DENER, V. ELJKHOUT, J. FAIBUSSOWITSCH, W. D.

- GROPP, V. HAPLA, T. ISAAC, P. JOLIVET, D. KARPEEV, D. KAUSHIK, M. G. KNEPLEY, F. KONG, S. KRUGER, D. A. MAY, L. C. MCINNES, R. T. MILLS, L. MITCHELL, T. MUNSON, J. E. ROMAN, K. RUPP, P. SANAN, J. SARICH, B. F. SMITH, H. SUH, S. ZAMPINI, H. ZHANG, H. ZHANG, AND J. ZHANG, *PETSc/TAO users manual*, Tech. Rep. ANL-21/39 - Revision 3.22, Argonne National Laboratory, 2024.
- [9] T. BLICKHAN, J. STRATTON, AND A. A. KAPTANOGLU, *MRX: A differentiable 3D MHD equilibrium solver without nested flux surfaces*, arXiv preprint arXiv:2510.26986, (2025).
- [10] F. BREZZI, J. DOUGLAS, AND L. D. MARINI, *Two families of mixed finite elements for second order elliptic problems*, *Numerische Mathematik*, 47 (1985), pp. 217–235.
- [11] S. CANDELARESI, D. PONTIN, AND G. HORNIG, *Mimetic methods for Lagrangian relaxation of magnetic fields*, *SIAM Journal on Scientific Computing*, 36 (2014), pp. B952–B968.
- [12] S. CANDELARESI, D. I. PONTIN, AND G. HORNIG, *Magnetic field relaxation and current sheets in an ideal plasma*, *The Astrophysical Journal*, 808 (2015), p. 134.
- [13] Q. CHENG, C. LIU, AND J. SHEN, *A new Lagrange multiplier approach for gradient flows*, *Computer Methods in Applied Mechanics and Engineering*, 367 (2020), p. 113070.
- [14] Q. CHENG AND J. SHEN, *Global constraints preserving scalar auxiliary variable schemes for gradient flows*, *SIAM Journal on Scientific Computing*, 42 (2020), pp. A2489–A2513.
- [15] R. CHODURA AND A. SCHLÜTER, *A 3D code for MHD equilibrium and stability*, *Journal of Computational Physics*, 41 (1981), pp. 68–88.
- [16] I. J. D. CRAIG AND D. PONTIN, *Current singularities in line-tied three-dimensional magnetic fields*, *The Astrophysical Journal*, 788 (2014), p. 177.
- [17] I. J. D. CRAIG AND A. D. SNEYD, *A dynamic relaxation technique for determining the structure and stability of coronal magnetic fields*, *The Astrophysical Journal*, 311 (1986), pp. 451–459.
- [18] ———, *The Parker problem and the theory of coronal heating*, *Solar Physics*, 232 (2005), pp. 41–62.
- [19] L. B. DA VEIGA, K. HU, AND L. MASCOTTO, *Error estimates for a helicity-preserving finite element discretisation of an incompressible magnetohydrodynamics system*, *ESAIM: Mathematical Modelling and Numerical Analysis*, 59 (2025), pp. 1075–1094.
- [20] D. FARACO, S. LINDBERG, AND L. SZÉKELYHIDI JR, *Magnetic helicity, weak solutions and relaxation of ideal MHD*, *Communications on Pure and Applied Mathematics*, 77 (2024), pp. 2387–2412.
- [21] P. E. FARRELL, M. HE, K. HU, AND G. ZHANG, *Software used in ‘global and local helicity-preservation in finite element magnetic relaxation’*, 2026. [10.5281/zenodo.18837992](https://doi.org/10.5281/zenodo.18837992).
- [22] M. H. FREEDMAN, *A note on topology and magnetic energy in incompressible perfectly conducting fluids*, *Journal of Fluid Mechanics*, 194 (1988), pp. 549–551.
- [23] H. GARCKE, W. JIANG, C. SU, AND G. ZHANG, *Structure-preserving parametric finite element method for surface diffusion based on Lagrange multiplier approaches*, *SIAM Journal on Scientific Computing*, 47 (2025), pp. A1983–A2011.
- [24] H. GARCKE, D. TRAUTWEIN, AND G. ZHANG, *Structure-preserving parametric finite element methods for two-phase Stokes flow based on Lagrange multiplier approaches*, arXiv preprint arXiv:2508.12326, (2025).
- [25] E. S. GAWLIK AND F. GAY-BALMAZ, *A finite element method for MHD that preserves energy, cross-helicity, magnetic helicity, incompressibility, and $\operatorname{div} B = 0$* , *Journal of Computational Physics*, 450 (2022), p. 110847.
- [26] S. GUO, L. MEI, W. YAN, AND Y. LI, *Mass-, energy-, and momentum-preserving spectral scheme for Klein–Gordon–Schrödinger system on infinite domains*, *SIAM Journal on Scientific Computing*, 45 (2023), pp. B200–B230.
- [27] D. A. HAM, P. H. J. KELLY, L. MITCHELL, C. J. COTTER, R. C. KIRBY, K. SAGIYAMA, N. BOUZIANI, S. VORDERWUELBECKE, T. J. GREGORY, J. BETTERIDGE, D. R. SHAPERO, R. W. NIXON-HILL, C. J. WARD, P. E. FARRELL, P. D. BRUBECK, I. MARSDEN, T. H. GIBSON, M. HOMOLYA, T. SUN, A. T. T. MCRAE, F. LUPORINI, A. GREGORY, M. LANGE, S. W. FUNKE, F. RATHGEBER, G.-T. BERCEA, AND G. R. MARKALL, *Firedrake User Manual*, Imperial College London and University of Oxford and Baylor University and University of Washington, first edition ed., 5 2023.
- [28] M. HE, P. FARRELL, K. HU, AND B. ANDREWS, *Helicity-preserving finite element discretization for magnetic relaxation*, *SIAM Journal on Scientific Computing*, 48 (2025), pp. B165–B183.
- [29] K. HU, Y.-J. LEE, AND J. XU, *Helicity-conservative finite element discretization for incompressible MHD systems*, *Journal of Computational Physics*, 436 (2021), p. 110284.
- [30] K. HU, Y. MA, AND J. XU, *Stable finite element methods preserving $\nabla \cdot \mathbf{B} = 0$ exactly for MHD models*, *Numerische Mathematik*, 135 (2017), pp. 371–396.
- [31] K. HU AND J. XU, *Structure-preserving finite element methods for stationary MHD models*,

- Mathematics of Computation, 88 (2019), pp. 553–581.
- [32] I. C. F. IPSEN, *A note on preconditioning nonsymmetric matrices*, SIAM Journal on Scientific Computing, 23 (2001), pp. 1050–1051.
 - [33] F. LAAKMANN, K. HU, AND P. E. FARRELL, *Structure-preserving and helicity-conserving finite element approximations and preconditioning for the Hall MHD equations*, Journal of Computational Physics, 492 (2023), p. 112410.
 - [34] A. LONGBOTTOM, G. RICKARD, I. J. D. CRAIG, AND A. D. SNEYD, *Magnetic flux braiding: force-free equilibria and current sheets*, The Astrophysical Journal, 500 (1998), p. 471.
 - [35] Y. MA, K. HU, X. HU, AND J. XU, *Robust preconditioners for incompressible MHD models*, Journal of Computational Physics, 316 (2016), pp. 721–746.
 - [36] S. MAO AND R. XI, *An incompressibility, $\text{div}B=0$ preserving, current density, helicity, energy-conserving finite element method for incompressible MHD systems*, Journal of Computational Physics, 538 (2025), p. 114130.
 - [37] W. S. MASSEY, *Higher order linking numbers*, Journal of Knot Theory and Its Ramifications, 7 (1998), pp. 393–414.
 - [38] H. MOFFATT, *Magnetic relaxation and the Taylor conjecture*, Journal of Plasma Physics, 81 (2015), p. 905810608.
 - [39] M. F. MURPHY, G. H. GOLUB, AND A. J. WATHEN, *A note on preconditioning for indefinite linear systems*, SIAM Journal on Scientific Computing, 21 (2000), pp. 1969–1972.
 - [40] J.-C. NÉDÉLEC, *Mixed finite elements in \mathbb{R}^3* , Numerische Mathematik, 35 (1980), pp. 315–341.
 - [41] D. PONTIN, S. CANDELARESI, A. RUSSELL, AND G. HORNIG, *Braided magnetic fields: equilibria, relaxation and heating*, Plasma Physics and Controlled Fusion, 58 (2016), p. 054008.
 - [42] P.-A. RAVIART AND J.-M. THOMAS, *A mixed finite element method for 2-nd order elliptic problems*, in Mathematical Aspects of Finite Element Methods: Proceedings of the Conference Held in Rome, December 10–12, 1975, Springer, 2006, pp. 292–315.
 - [43] Y. SAAD, *A flexible inner-outer preconditioned GMRES algorithm*, SIAM Journal on Scientific Computing, 14 (1993), pp. 461–469.
 - [44] C. B. SMIET, S. CANDELARESI, AND D. BOUWMEESTER, *Ideal relaxation of the Hopf fibration*, Physics of Plasmas, 24 (2017), p. 072110.
 - [45] J. B. TAYLOR, *Relaxation of toroidal plasma and generation of reverse magnetic fields*, Physical Review Letters, 33 (1974), p. 1139.
 - [46] W. TONNON AND R. HIPTMAIR, *Semi-Lagrangian finite element exterior calculus for incompressible flows*, Advances in Computational Mathematics, 50 (2024), p. 11.
 - [47] A. WILMOT-SMITH, G. HORNIG, AND D. PONTIN, *Magnetic braiding and parallel electric fields*, The Astrophysical Journal, 696 (2009), p. 1339.
 - [48] ———, *Magnetic braiding and quasi-separatrix layers*, The Astrophysical Journal, 704 (2009), pp. 1288–1295.
 - [49] L. WOLTJER, *A theorem on force-free magnetic fields*, Proceedings of the National Academy of Sciences, 44 (1958), pp. 489–491.
 - [50] A. R. YEATES, *Magnetohydrodynamic relaxation theory*, in Topics in Magnetohydrodynamic Topology, Reconnection and Stability Theory, Springer, 2019, pp. 117–143.
 - [51] A. R. YEATES, *On the limitations of magneto-frictional relaxation*, Geophysical & Astrophysical Fluid Dynamics, 116 (2022), pp. 305–320.
 - [52] A. R. YEATES AND G. HORNIG, *Unique topological characterization of braided magnetic fields*, Physics of Plasmas, 20 (2013), p. 012102.
 - [53] A. R. YEATES, A. L. WILMOT-SMITH, AND G. HORNIG, *Topological constraints on magnetic relaxation*, Physical Review Letters, 105 (2010), p. 085002.
 - [54] Y. ZHANG, A. PALHA, M. GERRITSMAN, AND L. G. REBHOLZ, *A mass-, kinetic energy- and helicity-conserving mimetic dual-field discretization for three-dimensional incompressible Navier-Stokes equations, part I: Periodic domains*, Journal of Computational Physics, 451 (2022), p. 110868.
 - [55] Y. ZHANG, A. PALHA, M. GERRITSMAN, AND Q. YAO, *A MEEVC discretization for two-dimensional incompressible Navier-Stokes equations with general boundary conditions*, Journal of Computational Physics, 510 (2024), p. 113080.
 - [56] Y. ZHOU, Y.-M. HUANG, H. QIN, AND A. BHATTACHARJEE, *Formation of current singularity in a topologically constrained plasma*, Physical Review E, 93 (2016), p. 023205.
 - [57] ———, *Constructing current singularity in a 3D line-tied plasma*, The Astrophysical Journal, 852 (2017), p. 3.
 - [58] Y. ZHOU, H. QIN, J. W. BURBY, AND A. BHATTACHARJEE, *Variational integration for ideal magnetohydrodynamics with built-in advection equations*, Physics of Plasmas, 21 (2014).